



저작자표시-비영리-변경금지 2.0 대한민국

이용자는 아래의 조건을 따르는 경우에 한하여 자유롭게

- 이 저작물을 복제, 배포, 전송, 전시, 공연 및 방송할 수 있습니다.

다음과 같은 조건을 따라야 합니다:



저작자표시. 귀하는 원저작자를 표시하여야 합니다.



비영리. 귀하는 이 저작물을 영리 목적으로 이용할 수 없습니다.



변경금지. 귀하는 이 저작물을 개작, 변형 또는 가공할 수 없습니다.

- 귀하는, 이 저작물의 재이용이나 배포의 경우, 이 저작물에 적용된 이용허락조건을 명확하게 나타내어야 합니다.
- 저작권자로부터 별도의 허가를 받으면 이러한 조건들은 적용되지 않습니다.

저작권법에 따른 이용자의 권리는 위의 내용에 의하여 영향을 받지 않습니다.

이것은 [이용허락규약\(Legal Code\)](#)을 이해하기 쉽게 요약한 것입니다.

[Disclaimer](#)

A THESIS
FOR THE DEGREE OF MASTER OF SCIENCE

**Application of fourier transform infrared
(FT-IR) spectroscopy for rapid screening of
mutant lines in *Panax ginseng***

Javzandulam Ulziisaikhan

Department of Biotechnology

GRADUATE SCHOOL

JEJU NATIONAL UNIVERSITY

2016.08

**Application of fourier transform infrared (FT-IR) spectroscopy
for rapid screening of mutant lines in *Panax ginseng***

Javzandulam Ulziisaikhan
(Supervised by Professor Hyo-Yeon Lee)

A thesis submitted in partial fulfillment of the requirement for the degree of
Master of Science

2016.08

This thesis has been examined and approved by



.....
Chairperson of the supervising committees

Professor Hyeon-Jin Sun, Subtropical Horticulture Research Institute, Jeju National University



.....
Professor Dae-Hwa Yang, Subtropical Horticulture Research Institute, Jeju National University



.....
Professor Hyo-Yeon Lee, Faculty of Biotechnology, Jeju National University

Department of Biotechnology
GRADUATE SCHOOL
JEJU NATIONAL UNIVERSITY

A THESIS
FOR THE DEGREE OF MASTER OF SCIENCE

**Application of fourier transform infrared
(FT-IR) spectroscopy for rapid screening of
mutant lines in *Panax ginseng***

Javzandulam Ulziisaikhan

(Supervised by Professor Hyo-Yeon Lee)

Department of Biotechnology

GRADUATE SCHOOL

JEJU NATIONAL UNIVERSITY

2016. 08

CONTENTS

CONTENTS	1
ABBREVIATIONS	3
LIST OF FIGURES	4
LIST OF TABLES	7
SUMMARY	8
INTRODUCTION	9
MATERIALS AND METHODS	12
Plant material.....	12
Chemical constitution of culture medium.....	12
Condition of petri dish culture.....	13
Gamma irradiation.....	13
Preparation of FT-IR whole-cell extract.....	14
Spectral data procession of FT-IR spectroscopy.....	14
Multivariate statistical analysis.....	15
Preparation of the crude ginsenoside extract	15
Ginsenoside Rg1, Re, Rc, Rb1, Rb2, Rd determination by HPLC.....	17
Statistical analysis.....	20

RESULTS	21
Effects of gamma irradiation on survival rate of adventitious roots	21
Rapid discrimination of large number of mutant ginseng roots by FT-IR spectroscopy.....	23
Quantitative prediction of ginsenoside content in ginseng mutant lines by PLS regression modeling.....	24
CONCLUSIONS	48
REFERENCES	49
ACKNOWLEDGEMENT	55

ABBREVIATIONS

NAA	Naphthalene acetic acid
IAA	Indole-3-acetic acid
JA	Jasmonic acid
FT-IR	Fourier transform infrared spectroscopy
PC	Principle compound
PCA	Principal component analysis
PLS-DA	Partial least squares-discriminant analysis
HPLC	High performance liquid chromatography
HPLC-PDA	High performance liquid chromatography-photodiode array detector
ACN	Acetonitrile
MS	Murashige & Skoog
PPD	Protopanaxadiol
PPT	Protopanaxatriol
UV	Ultraviolet
Gy	Gray
2,4-D	2,4-dichlorophenoxy-acetic acid

LIST OF FIGURES

- Figure 1. Adventitious roots generated from Korean wild ginseng (*P.ginseng* Meyer).
- Figure 2. Procedure of the crude ginsenoside extraction for HPLC analysis.
- Figure 3. Effect of gamma irradiation on *P.ginseng* adventitious roots.
- Figure 4. Survival rate among the gamma irradiated adventitious roots.
- Figure 5. Representative FT-IR spectrum from 10Gy radiation mutant lines and wild type.
- Figure 6. Two-dimensional PCA score plot of FT-IR spectral data from 10Gy radiation mutant lines and wild type.
- Figure 7. PC loading values plot based on PCA score plot data of 10Gy radiation mutant lines and wild type.
- Figure 8. Determination of ginsenoside contents from 10Gy mutant lines and wild type control by HPLC analysis.
- Figure 9. Linear regression plot between predicted and estimated values of total ginsenoside content of 10Gy mutant ginseng.
- Figure 10. Linear regression plot between predicted and estimated values of ginsenoside Rb1 content of 10Gy mutant ginseng.
- Figure 11. Linear regression plot between predicted and estimated values of ginsenoside Re+Rg1 content of 10Gy mutant ginseng.
- Figure 12. Linear regression plot between predicted and estimated values of ginsenoside Rc content of 10Gy mutant ginseng.

Figure 13. Linear regression plot between predicted and estimated values of ginsenoside Rb2 content of 10Gy mutant ginseng.

Figure 14. Linear regression plot between predicted and estimated values of ginsenoside Rd content of 10Gy mutant ginseng.

Figure 15. Representative FT-IR spectrum from 30Gy radiation mutant lines and wild type

Figure 16. Two-dimensional PCA score plot of FT-IR spectral data from 30Gy radiation mutant lines and wild type.

Figure 17. PC loading values plot based on PCA score plot data of 30Gy radiation mutant lines and wild type.

Figure 18. Determination of ginsenoside contents from 30Gy mutant lines and wild type control by HPLC analysis.

Figure 19. Linear regression plot between predicted and estimated values of total ginsenoside content of 30Gy mutant ginseng.

Figure 20. Linear regression plot between predicted and estimated values of ginsenoside Rb1 content of 30Gy mutant ginseng.

Figure 21. Linear regression plot between predicted and estimated values of ginsenoside Re+Rg1 content of 30Gy mutant ginseng.

Figure 22. Linear regression plot between predicted and estimated values of ginsenoside Rc content of 30Gy mutant ginseng.

Figure 23. Linear regression plot between predicted and estimated values of ginsenoside Rb2 content of 30Gy mutant ginseng.

Figure 24. Linear regression plot between predicted and estimated values of ginsenoside Rd content of 30Gy mutant ginseng.

LIST OF TABLES

Table 1. Instrumental conditions of HPLC for ginsenoside Re, Rg1 ,Rb1, Rb2, Rc, Rd analysis.

Table 2. HPLC solvent condition for ginsenoside Re, Rg1 ,Rb1, Rb2, Rc, Rd analysis.

Table 3. Ginsenoside contents of 10Gy mutagenized ginseng cell lines as determined by HPLC.

Table 4. Ginsenoside contents of 30Gy mutagenized ginseng cell lines as determined by HPLC.

SUMMARY

Panax ginseng Meyer, an important pharmaceutical herb that is extensively cultivated in Japan, China and Korea. Ginseng has been used as a medicine for over 2000 years in these oriental regions. However its use has been rapidly expanding in Western countries as the demand for complementary and alternative medicine rises (Shim *et al.* 2009). Saponins are glycosylated triterpenes, referred to ginsenoside, have been especially noted as active compounds contributing to the various efficacy of ginseng. In the present study adventitious roots of *P.ginseng* were treated by different dosages of gamma irradiation zero being non-irradiated, 10Gy, 30Gy, 50Gy and 70Gy, grown in hormone free MS modified medium at $23\pm 2^{\circ}\text{C}$ dark condition for 7 days. The effects of gamma radiation on adventitious root was done by checking the remaining survived roots after 5 weeks of exposure. Total 137 mutagenized ginseng lines including wild type survived after gamma irradiation. Hence out of 137 mutant lines corresponding to the three wild-type lines and only 81 (10Gy), 39 (30Gy) mutagenized lines were selected for FT-IR analysis. An efficient selection system has been established that is suitable to quantify the contents of ginsenoside in ginseng mutant lines using Fourier transform infrared (FT-IR) spectroscopy in junction with multivariate analysis. The quantitative prediction modeling of ginsenoside content from mutant ginseng lines was established using partial least square regression algorithms (PLS-DA) from FT-IR spectra data and ginsenoside contents measured by HPLC analysis. The correlation coefficient (R^2) for ginsenoside Re+Rg1, Rb1, Rb2, Rc, Rd and total ginsenoside contents between predicted and estimated values measured by linear regression analysis was $R=0.99$, respectively. The ginsenoside contents prediction modeling could be used as an efficient tool for selection of elite mutant lines with high ginsenoside contents in mutation breeding of *P.ginseng*.

INTRODUCTION

P.ginseng Meyer (Korean wild ginseng) is one of the medicinally, economically important perennial herbaceous, aromatic herb with short underground rhizome interrelated with fleshy white root (Lui *et al.* 2008, Xie *et al.* 2011). There are more than 40 different ginsenoside producing various pharmacological effects have been isolated and identified from ginseng roots (Fuzzati 2004). The underground part have as a higher amounts of ginsenoside Rb1, Rc and Rg1, on the other hand above ground parts have as a higher amounts of ginsenoside Rd, Re, and Rg1 (Peigen 1989). Ginseng saponin referred to as a ginsenoside are categorized into dammarane (protopanaxadiol-PPD, protopanaxatriol-PPT) and oleanane type based on their aglycone structure (Fuzzati *et al.* 1999). The contents of the ginsenoside can affect the immune system, central nervous system, cardiovascular system and the endocrine system in a large number of ways. This mainly contributed to the species, growth condition and location etc. The active ingredients promote immune function, increase the secretion of endocrine and have anti-aging as well as anti-stress effects (Briskin 2000, Shibata 2001, Vogler *et al.* 1999, Kim *et al.* 2003). It is difficult to produce large quantities of root in the field due to the inevitable limitations of the *P.ginseng* breeding (Han *et al.* 2009). There have been alternative methods created to counter the complications posed from producing ginsenoside from its natural source. Some of these attempts include; using classical tissue culture system (Wu *et al.* 1999, Zhang *et al.* 2014), bioreactor culture system (Sivakumar *et al.* 2005), *Agrobacterium*-mediated hairy root production (Mallol *et al.* 2001, Yoshikawa *et al.* 1987) and mutation breeding by gamma irradiation (Kim *et al.* 2009, Kim *et al.* 2013, Zhang *et al.* 2011). Besides, jasmonic acid (JA) is an effective elicitor for secondary metabolite induction in plant cell cultures (Ketchum *et al.* 1999).

Lately, radiation technology has been widely applied in the various field such as clinical research, crop research and tissue engineering. Radiation energy is the utility tool to improve the functional constitution of crop field (Ayed *et al.* 1999). In addition, the ionizing energy considerably affects the antioxidant properties by inducing structural changes in the plants components; however several studies have shown that gamma irradiation can also degrade glycosidic bond linkage and protein structures (Ananthaswamy *et al.* 1970, Sokhey *et al.* 1993, Charlesby 1981, Deschreider 1960). Plants can be affected by ionizing radiation in various ways. These include altering sugars, damaging DNA, forming DNA-DNA and DNA-protein crosslinks, as well as causing single and double strand breaks (Kovalchuk *et al.* 2007, Rakwal *et al.* 2009). Recently, numerous researchers have achieved mutation breeding by ionizing irradiation. Kim *et al.* (2005) reported that high levels of amino acids were obtained from mutant rice lines. Mutation breeding of plants is considered to be an effective method for improving the variety of crop production. Gamma irradiation, among several other methods, is used for crop improvement programs across several species. Recent reports showed that mutagenesis by gamma irradiation gained accelerating growth in intensified ginsenoside production of *P.ginseng* (Kim *et al.* 2009). In maize, grain yields for irradiated samples show an increase above non-irradiated samples for doses up to about 250Gy with an optimal yield at a dose of 150Gy. A corresponding increase for groundnut is observed for doses up to about 930Gy, 300Gy doses result in an optimum yield (Mokobia *et al.* 2006). At a rate of 100Gy, grain yield of maximum generation in barley was observed (Subhan *et al.* 2004). Latest reports revealed that mutagenesis by gamma irradiation gained rapid development in enhanced ginsenoside manufacturing of *P.ginseng*. Mutant cell lines generated by gamma irradiation on *P.ginseng* have been mainly selected on the phenotypic morphology and ginsenoside content using by HPLC analysis (Kim *et al.* 2009, Kim *et al.* 2013, Zhang *et al.* 2011).

Ginseng is very complicated mixture than other herbal medicines. The modern analytical technologies such as thin-layer chromatography (TLC), tandem instrumentation of liquid chromatography with mass spectrometry (LC/MC) and high-performance liquid chromatography (HPLC) etc, were applied to identify and differentiate the ginseng crude drug and products based on the chemical components such as ginsenoside. Unfortunately, all of these methods have disadvantages which are time-consuming, labour-intensive, expensive and requiring a large quantitative of organic solvent and sample (Lai *et al.* 2010, Chew *et al.* 2004). Fourier transform infrared (FT-IR) spectroscopy has become an useful method in the process of screening mutant cell lines in plant breeding, being simple and rapid analytical method. In terms of convenient usage of technique, favorable effects, brief data obtainment time and a small amount of samples needed, Fourier transform infrared (FT-IR) spectroscopic method has been many advantageous for the classification of herbal medicine. Unfortunately, studies concerning and including FT-IR techniques are still under development (Chen *et al.* 2008, Yap *et al.* 2007). FT-IR is commonly worked in combination with chemometrics for various plant research applications, including classification between plant species (Kim *et al.* 2004) and cultivars (Song *et al.* 2014), screening for cell-wall mutant (Chen *et al.* 1998) and quantitative prediction of functional compounds (Kwon *et al.* 2015). In herbal medicines, a FT-IR spectrum contains multiple overlapping absorption bands depicting the various modes of vibration of a large number of molecular constituents in the compounds (Yin *et al.* 2015). These vibrational bands, which can be detected at low levels, are sensitive to the chemical and physical states of the compounds (Lai *et al.* 2010). In this study, we induced mutant roots of *P.ginseng* that had been mutagenized by gamma rays and developed a quantitative prediction modeling for ginsenoside contents from FT-IR spectra of ginseng mutant cell lines.

MATERIALS AND METHODS

Plant material

Adventitious roots obtained from Korean wild ginseng. The following images consist of adventitious roots from Korean ginseng (Kim *et al.* 2003) which have been maintained for more than ten year duration in Subtropical Horticulture Institute of Jeju National University (Figure 1).

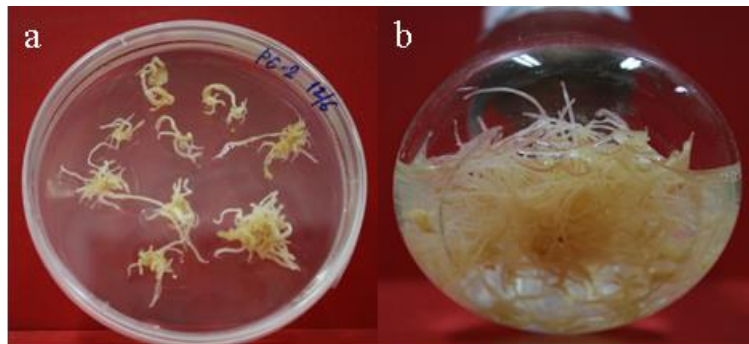


Figure 1. Adventitious roots generated from Korean wild ginseng (*P.ginseng* Meyer). Petri dish culture (a), Flask culture (b).

Chemical constitution of culture medium

P.ginseng adventitious roots generated on Murashige and Skoog (MS, 1962) medium as follows (mg/L): NH_4NO_3 (687.5), KNO_3 (1900), KH_2PO_4 (170), H_3BO_3 (6.2), $\text{MnSO}_4 \cdot 4\text{H}_2\text{O}$ (23.3), $\text{ZnSO}_4 \cdot 7\text{H}_2\text{O}$ (8.6), KI (0.83), $\text{Na}_2\text{MoO}_4 \cdot 2\text{H}_2\text{O}$ (0.25), $\text{CuSO}_4 \cdot 5\text{H}_2\text{O}$ (0.025), $\text{CoCl}_2 \cdot 6\text{H}_2\text{O}$ (0.025), $\text{CaCl}_2 \cdot 2\text{H}_2\text{O}$ (440), $\text{MgSO}_4 \cdot 7\text{H}_2\text{O}$ (370), Na_2EDTA (37.3), $\text{FeSO}_4 \cdot 7\text{H}_2\text{O}$

(27.8), Nicotinic acid (5), Pyridoxine Hydrochloride (1), Thiamine Hydrochloride (2.5), Glycine (2). Supplemented with 10.87 μ mol Naphthalene acetic acid (NAA), 1.43 μ mol Indole-3-acetic acid (IAA) and 3% sucrose. Before sterilization culture medium was adjusted to pH=6.0 autoclaved at 121°C and 1.2 Kg/cm² pressure for 15 min.

Condition of petri dish culture

Adventitious roots were cut into ten to twenty mm pieces. These were cultured in petri dish (10cm in diameter, 1.5 cm in height) with a lid containing 50 mL MS solid medium. This was sealed with a wrap (Advantec, USA) and cultured in dark conditions at 23 \pm 2°C. The induced mutant adventitious roots were sub-cultured every 3 weeks intervals on the same medium for maintenance.

Gamma irradiation

Radioactive substances give out radiation all of the time. Alpha, beta and gamma are the three types of nuclear radiation. Alpha is the least penetrating, while gamma is the most penetrating. Nonetheless, all three are ionizing radiation they can knock electrons out of atoms and form charged particles. Adventitious roots (10-20mm) were placed in plastic petri dishes (ten pieces per petri dish), grown at 23 \pm 2°C and cultured for 5 days in 3% sucrose of MS medium without NAA and IAA.

They were brought into contact with gamma radiation from cobalt (⁶⁰Co) source applying a gamma radiation apparatus at the Institute for Nuclear Science and Technology, Jeju National University. Irradiation dosages were 0 (non-irradiated), 10Gy, 30Gy, 50Gy and 70Gy. For each quantity, three petri dishes of the samples were exposed in triplicate.

Survival rate among of gamma irradiated adventitious roots were evaluated by measuring the number of survival adventitious roots after 5 weeks culture.

Preparation of FT-IR whole-cell extract

Root samples were dried for 72 hours at 38⁰C and freeze-dried for 48 hours at -80⁰C, ground into powders, and stored at -80⁰C before analysis. A total 123 mutant line of adventitious root samples were analyzed in this study. Crude ginseng whole-cell extracts were prepared for FT-IR analysis. Twenty milligrams of each ginseng root powder was mixed with 200 μ L of extraction buffer 20% (v/v) methanol in a 1.5 mL Eppendorf tube, combined vigorously, and incubated in a 50⁰C water bath for 10 min with regular vortexing. Suspension were centrifuged at 13,000 rpm for 5 min, and supernatants were transferred to fresh tubes. Centrifugation was repeated when cell debris was not fully removed. These crude whole-cells extracts from ginseng roots stored at -20⁰C prior to FT-IR spectroscopy analysis.

Spectral data procession of FT-IR spectroscopy

For FT-IR spectroscopy analysis, five μ L aliquots of prepared crude ginseng whole-cell extracts were loaded in a 384 well ZnSe plate and dried on a hotplate at 37⁰C. After the samples were dried, the 384 ZnSe plate was placed in a micro plate reader unit HTS-XT (Bruker Optics GmbH, Ettlingen, Germany).

The spectrum of each samples were recorded scans at a resolution of 4 cm^{-1} in the range of 4,000 cm^{-1} to 400 cm^{-1} . Signal-to-noise ratio was improved by co-addition of 128 interferograms and averaging with the analytical results. For multivariate analysis, original

(raw) FT-IR spectra were preprocessed accounting for baseline corrections, spectral intensity normalization and smoothing by OPUS lab (version 6.5, Bruker, Ettlingen, Germany). Nine spectra were recorded from each samples for statistical analysis.

Multivariate statistical analysis

For multivariate analysis, the 1,800-800 cm^{-1} region of the FT-IR spectral data was subjected to multivariate analysis, instead of the full spectrum. The preprocessed FT-IR spectral data were imported into the R statistical analysis program (version 2.15.0, R Development Core Team) for principal component analysis. PCA was conducted using a non-linear iterative partial least squares (NIPALS) algorithm (Wold 1966). Scores extracted from PCA analysis were used to calculate the correlation matrices. We examined PC score loading values.

Preparation of the crude ginsenoside extract

Ginsenoside extraction and determination were carried out by modifying the method of Kwon *et al.* (2003). This method is currently being used in the Jeju National University (Zhang *et al.* 2011). Ultrasound-assisted extraction was performed using an ultrasonic water bath (Branson Ultrasonics, USA). The frequency is 50/60Hz and the output power is 117 volts. Extraction of crude ginsenoside from mutagenized adventitious roots of different lines conducted as follows (Figure 2). Dried 1000 mg sample powder was placed into a 100 mL conical flask with 30 mL of 80% (v/v) methanol and 20% water was added.

Then the flask was sonicated for 1 hour in an ultrasonic water bath. The extract obtained was evaporated using a rotary evaporator under a vacuum at 55C⁰. The evaporated residue (total extract yield) was dissolved in 20 mL of distilled water and washed twice, using a separatory funnel, with 20 mL of diethyl ether to remove the fat contents. The aqueous layer was extracted four times with 20 mL of water-saturated n-butanol. To remove impurities the butanol solution was washed twice with 30 mL of distilled water, thereby obtaining crude ginsenoside. The remaining butanolic solution was transferred to the tarred round bottom flask for evaporation using a rotary evaporator under vacuum at 55C⁰.

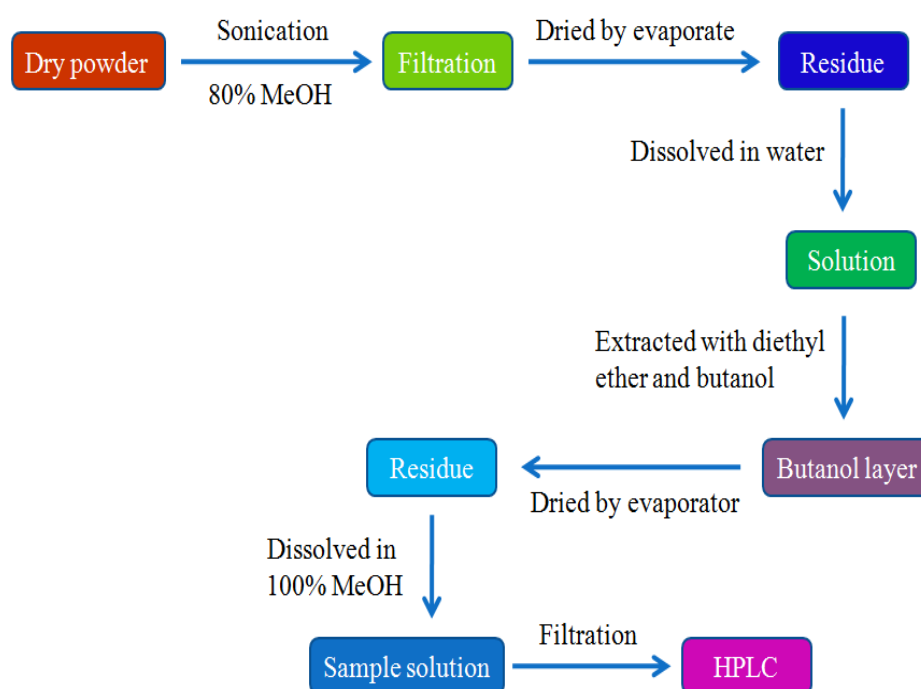


Figure 2. Procedure of the crude ginsenoside extraction for HPLC analysis

Ginsenoside Rg1, Re, Rc, Rb1, Rb2, Rd content determination by HPLC

Due to its sensitivity and adaptability to non-volatile polar compounds, HPLC is ideal for the analysis of saponins and sapogenins (Fuzzati 2004). The HPLC conditions for ginsenoside assay was slightly modified the previous report (Park et al. 2007). Quantitative determinations were achieved by HPLC using a Capcell-pak C18 MG (4.6 × 250 mm) column (Shiseido, Japan), Shimadzu detector (DGU-20A, LC-20AD, SIL-20A, CTO-20A, SPD-M20A, CBM-20A) (Table 1). HPLC grade methanol, acetonitrile, ethyl ether and 1-buthanol were obtained from Fisher Scientific (Korea). The water used in this study was treated with a Milli-Q water purification system (Millipore, USA). HPLC solvent condition for ginsenoside Re, Rg1, Rb1, Rb2, Rc, Rd analysis was displayed in (Table 2). Ginsenoside Rg1, Re, Rc, Rb1, Rd and Rb2 standards were purchased from BTGin Co., Ltd (Daejeon, Korea). Digoxin was used as internal standard. The total ginsenoside content was calculated as the sum of individual ginsenoside contents.

Table 1. Instrumental conditions of HPLC for ginsenoside Re, Rg1, Rb1, Rb2, Rc, Rd analysis.

Parameter	Condition
Instruments	Shimadzu HPLC system (DGU-20A, LC-20AD, SIL-20A, CTO-20A, SPD-M20A, CBM-20A)
Column	Capcell-pak C18 MG (4.6 × 250 mm) column, 5 μm (Shiseido, Japan)
Mobile phase	Distilled water and Acetonitrile
Flow rate	1ml/min
Photo Diode Array detector	Wavelength: 203 nm (PDA)
Scan wavelength	192 - 400 nm
Column temperature	35°C
Sample injection	10 μl
Run time	60 min

Table 2. HPLC solvent condition for ginsenoside Re, Rg1, Rb1, Rb2, Rc, Rd analysis.

Retention time (min)	Solvent (A)	Solvent (B)
0	80	18
22	70	30
32	55	45
50	50	50
55	82	18
60	82	18

Solvent (A): Distilled water, Solvent (B): Acetonitrile.

Standard solutions for the ten milligrams of each ginsenoside Rb1, Rc, Rb2, Rg1, Re and Rd were separately dissolved in five ml of 100% methanol. Diluted standard solution was maintained at -20C until 30 min before use and placed at room temperature to thermally equilibrate the solution. Digoxin stock solution was prepared in 80% methanol. Working solutions were prepared in methanol by mixing known quantities of ginsenoside. Five concentrations were made for standard curves; each concentration was 60, 120, 240, 320, 480 ppm respectively. Ginsenoside were detected at a wavelength of 203 nm with the peak areas corresponding to ginsenoside from the samples which matched retention times for authentic ginsenoside standards. The total ginsenoside content was measured by the amount of individual ginsenoside fractions.

The ginsenoside content of ginseng adventitious roots was calculated as follows:

(GC: ginsenoside content; SGC: sample ginsenoside concentration from HPLC; SV: sample volume; AR: adventitious root)

$$GC(\text{mg g}^{-1}) = \frac{SGC(\text{from HPLC})(\text{mg g}^{-1}) \times SV(\text{l})}{AR(\text{g})}$$

Statistical analysis

All of the experiments were conducted in three replicates. The statistical analysis was produced according to the SPSS system.

RESULTS

Effects of gamma irradiation on survival rate of adventitious roots

Firstly, we determined the survival rate of the *P.ginseng* adventitious roots at different dosage 0 (non-irradiated), 10Gy, 30Gy, 50Gy, 70Gy of gamma irradiation in this experiment. A mutant adventitious root lines were generated from the wild type adventitious roots by gamma irradiation as described previously (Zhang *et al.* 2011). Ten pieces (10-20mm) of wild type adventitious roots were placed on independent petri dish and were treated to 0 (non-irradiated), 10Gy, 30Gy, 50Gy, 70Gy of gamma ray (Figure 3). The survival rate of *P.ginseng* adventitious roots was decreased when gamma irradiation dosage increased.

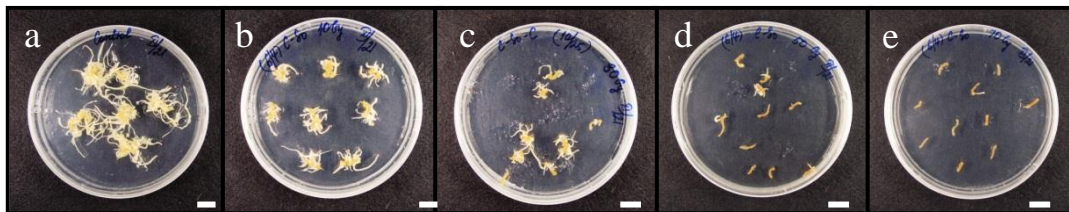


Figure 3. Effect of gamma irradiation on *P.ginseng* adventitious roots. Adventitious root of *P.ginseng* were placed on Murashige and Skoog (MS) solid medium with 2 mg/L NAA, 1 mg/L IAA and 3% sucrose at $23 \pm 2^\circ\text{C}$ in dark conditions. Adventitious root were irradiated with control (a), 10Gy, 30Gy, 50Gy, and 70Gy (b-e), respectively. Bar=1 cm

After treatment totally 137 gamma irradiated adventitious root lines had been survived including of control, 10Gy (81 lines) 93%, 30Gy (39 lines) 31%, 50Gy (10 lines) 3% and 70Gy (4 lines) 1.33% (Figure 4). For FT-IR analysis, 3 wild-type lines and 120 mutagenized lines 10Gy and 30Gy samples are used. *P.ginseng* hairy roots growth was suppressed by over 30Gy of ⁶⁰CO gamma ray (Choi *et al.* 2002). Gamma irradiation mediated mutagenesis of whole plants as well as roots yielding significant variations among the different mutated species and 50Gy of gamma ray was determined to be the optimal dose for inducing mutations (Joseph *et al.* 2004). *P.ginseng* was exposed through gamma irradiation and cell lines were selected by the higher growth ratio at 30Gy (Kim *et al.* 2009).

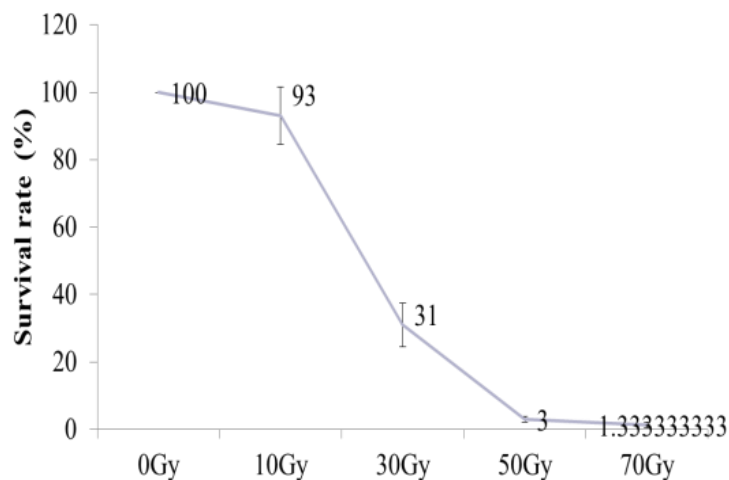


Figure 4. Survival rate among the gamma irradiated adventitious roots, was evaluated by measuring the number of surviving adventitious roots after 5 weeks of culturing in a hormone free MS medium. Bars indicate \pm SD of three replicates.

Rapid discrimination of large number of mutant ginseng roots by FT-IR spectroscopy

Large sets of data are analyzed using PCA. Principal components are smaller number of dimensions which are a result of the PCA procedure extracting information of the original data matrix. The differences or complexity of the data-set influences the number of principal components created. As the number of principal compounds increase, the variance defined by each principle compound decrease. The inherent data structure and underlying features that facilitate the identification of similarities and differences between materials is exposed by the PCA. The principle compounds which have the loadings spectra, present information on the contribution of the spectral regions to the differentiation between samples visible in the scores plot. For principal component analysis (PCA), the second derivative of each spectrum was calculated with 13 smoothing points in OPUS 7. The potential of FT-IR spectroscopy in combination with PCA to discriminate between different ginseng cell lines is evaluated. The FT-IR spectra of wild-type 10Gy and 30Gy mutagenized ginseng cell lines obtained from *P.ginseng* are presented in (Figure 5, Figure 15). The spectral variation was observed in the carbohydrate region ($1,150-950\text{ cm}^{-1}$), phospholipid, DNA and RNA region ($1,500-1,300\text{ cm}^{-1}$), protein and amide region ($1,700-1,550\text{ cm}^{-1}$) of the FT-IR spectra from ginseng cell lines (Figure 5, Figure 15). These spectral variations from ginseng cell lines suggest that there were quantitative and qualitative metabolic changes among the ginseng cell lines. The PCA of FT-IR data was displayed in a two-dimensional plot between ginseng cell lines using the first two principal components, PC 1 and PC 2. The 10Gy, 30Gy mutant lines scores scatter plot of the first two principal components PC 1 and PC 2, which together explain 17.5% (10Gy), 15.4% (30Gy) of variability (Figure 6, Figure 16), respectively. The 10Gy and 30Gy mutant lines scores are mainly scattered along PC 1 axis. Wild-type ginseng lines were located the positive side of PC 1 axis (10Gy) but wild-type ginseng lines placed the positive side of PC 2 axis (30Gy), whereas the 10Gy, 30Gy mutagenized ginseng lines

were broadly located in PC 1 axis from positive side to negative side. To identify the critical region of the FT-IR spectra for sample separation, a PC score loading values were examined. Significant FT-IR spectral variables for determining PC 1 and PC 2 were mostly distributed in the protein and amide region (1,700-1,500 cm^{-1}) and carbohydrate region (1,150-1,000 cm^{-1}) of the FT-IR spectra (Figure 7, Figure 17). These results conclude that qualitative and quantitative metabolic differences synonymous to carbohydrates and protein and amide regions are important for metabolic discriminations and evaluations between different ginseng cell lines.

Quantitative prediction of ginsenoside content in ginseng mutant lines by PLS regression modeling

The content of ginsenoside in the ginseng cell lines was measured by HPLC analysis as the reference data for further models using 10Gy (Table 3) and 30Gy (Table 4). A wild-type sample and randomly selected 27 (10Gy), 18 (30Gy) mutagenized cell lines were tested out by HPLC analysis. The total ginsenoside value was expressed as the sum of each ginsenoside in the ginseng cell lines. The total ginsenoside content of wild-type ginseng line was 3.80 mg/g, whereas the 10Gy irradiated mutant ginseng lines contained in broad ranges of total ginsenoside content from 1.27 mg/g up to 9.66 mg/g (Figure 8). As for 30Gy irradiated mutant ginseng lines contained 3.31 mg/g up to 8.69 mg/g ginsenoside (Figure 18). PLS model was developed in order to predict of ginsenoside content in mutagenized ginseng cell lines from FT-IR spectra. Quantitative prediction modeling of ginseng cell lines was established using PLS regression algorithm from FT-IR spectra data and ginsenoside contents measured by HPLC analysis. Satisfactory correlations between the predicted and estimated values of ginsenoside contents were found.

The correlation coefficients values for each ginsenoside 10Gy (Figure 10, Figure 11, Figure 13, Figure 14), 30Gy (Figure 20, Figure 21, Figure 22, Figure 23, Figure 24) were $R^2=0.99$ and for total ginsenoside 10Gy (Figure 9), 30Gy (Figure 19) was also $R^2=0.99$. These results reveal that the quantitative ginsenoside content could be carefully predicted from FT-IR spectra data of ginseng cell lines with sharp accuracy. The results were expressed as means followed by standard deviations.

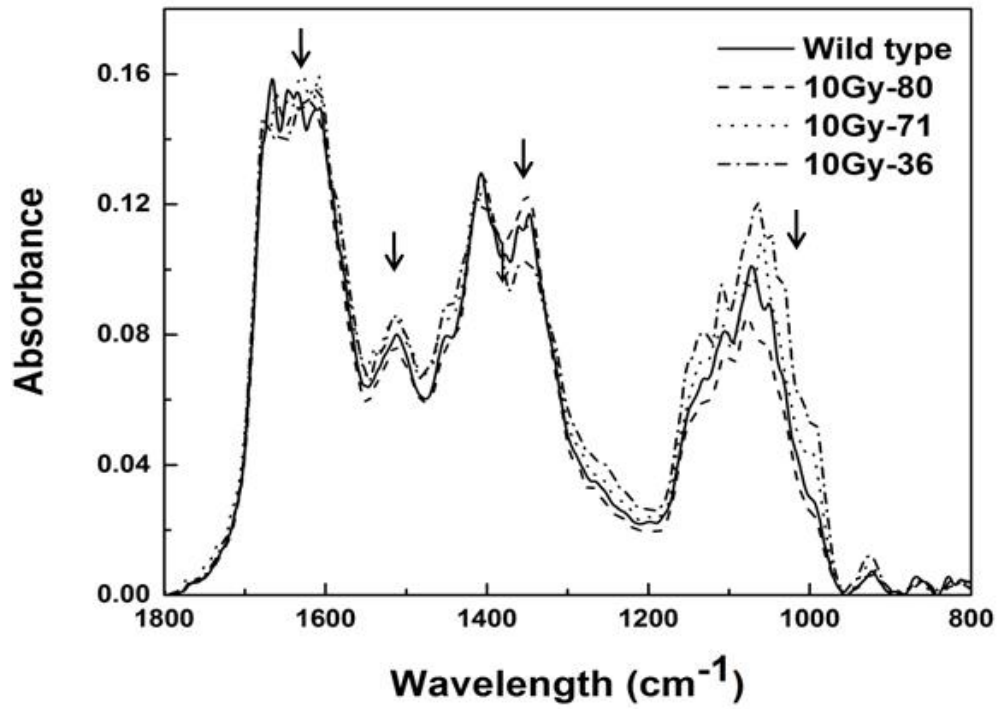


Figure 5. Representative FT-IR spectrum from 10Gy radiation mutant lines and wild type. Dotted and dashed lines represent 10Gy mutant lines and arrows signal the FT-IR regions displaying significant spectral variations .

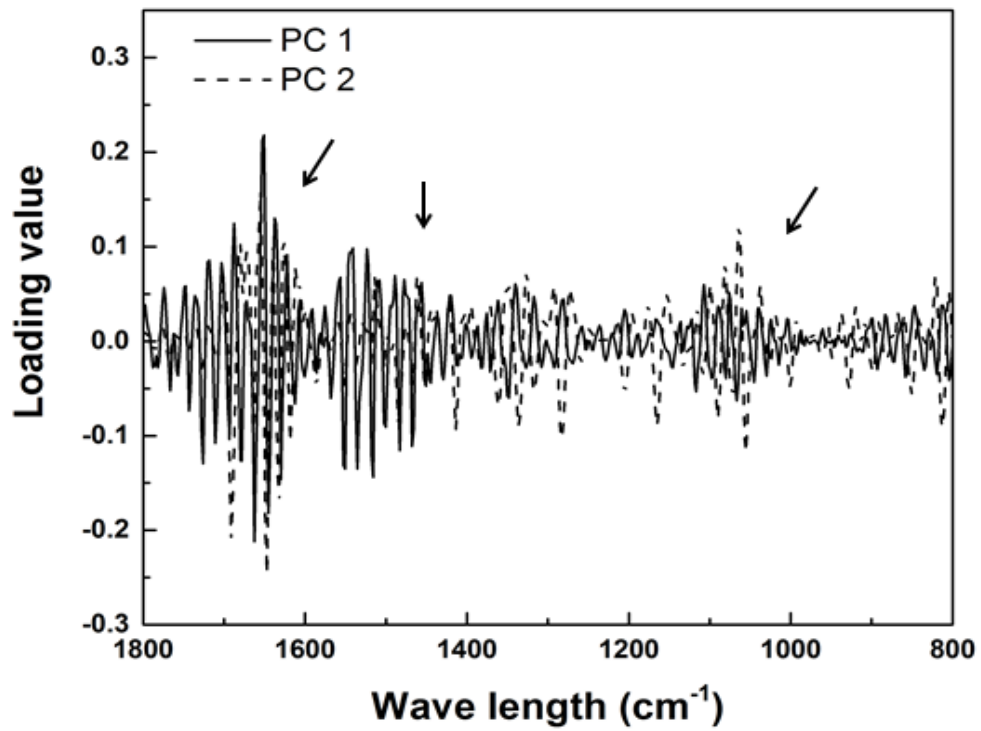


Figure 7. PC loading values plot based on PCA score plot data of 10Gy radiation mutant lines and wild type. The solid line represents the PC1 score and dotted line represents the PC 2 score. Arrows indicate the FT-IR regions which play important roles in ginseng mutant lines.

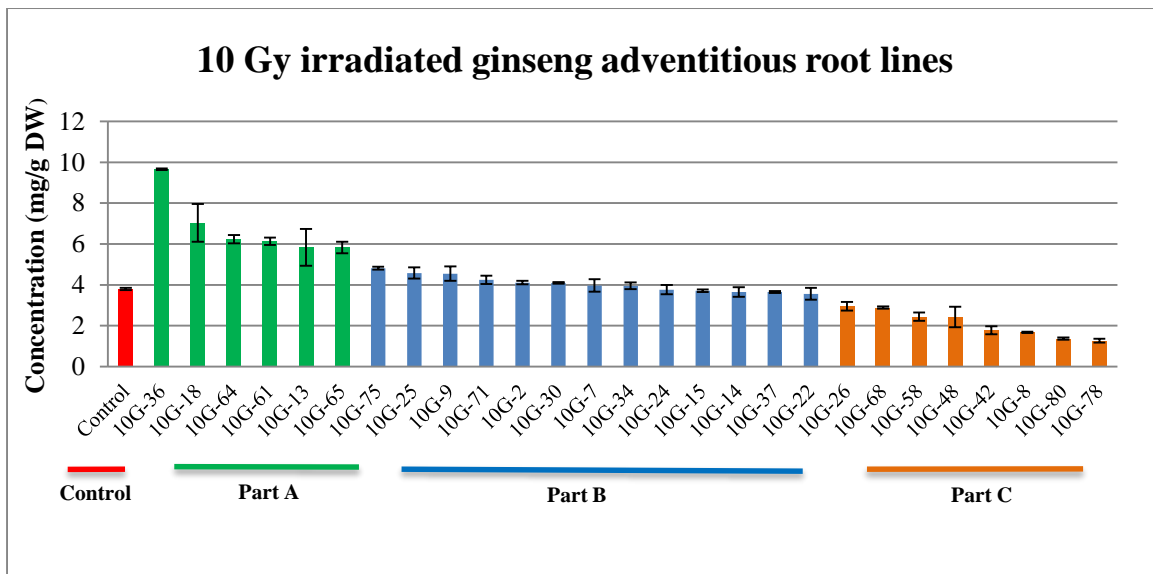


Figure 8. Determination of ginsenoside contents from 10Gy mutant lines and wild type control by HPLC analysis. Bars refer to \pm SD mean.

Table 3. Ginsenoside contents of 10Gy mutagenized ginseng cell lines as determined by HPLC. The results represent the means \pm SD, all samples were measured in three replicates.

Ginsenoside content (mg/g dry weight)						
Mutant line	Re+Rg1	Rb1	Rc	Rb2	Rd	Total ginsenoside
Control	2.13 \pm 0.15	0.34 \pm 0.12	0.22 \pm 0.05	0.25 \pm 0.09	0.83 \pm 0.01	3.80 \pm 0.06
10G-2	2.54 \pm 0.09	0.80 \pm 0.02	0.24 \pm 0.01	0.37 \pm 0.05	0.17 \pm 0.01	4.11 \pm 0.09
10G-7	1.75 \pm 0.08	0.41 \pm 0.05	1.37 \pm 0.32	0.33 \pm 0.01	0.08 \pm 0.01	3.97 \pm 0.30
10G-8	1.17 \pm 0.03	0.23 \pm 0.04	0.06 \pm 0.01	0.13 \pm 0.02	0.08 \pm 0.002	1.68 \pm 0.03
10G-9	2.39 \pm 0.58	0.92 \pm 0.09	0.38 \pm 0.02	0.52 \pm 0.01	0.57 \pm 0.05	4.55 \pm 0.36
10G-13	3.53 \pm 0.87	0.57 \pm 0.09	1.16 \pm 0.16	0.62 \pm 0.11	0.14 \pm 0.06	5.84 \pm 0.90
10G-14	2.39 \pm 0.04	0.59 \pm 0.03	0.14 \pm 0.02	0.44 \pm 0.18	0.11 \pm 0.02	3.65 \pm 0.23
10G-15	2.02 \pm 0.11	0.56 \pm 0.003	0.71 \pm 0.01	0.33 \pm 0.03	0.06 \pm 0.01	3.72 \pm 0.06
10G-18	4.67 \pm 0.88	1.03 \pm 0.05	0.35 \pm 0.06	0.69 \pm 0.08	0.16 \pm 0.05	7.04 \pm 0.92
10G-22	2.33 \pm 0.04	0.31 \pm 0.12	0.37 \pm 0.22	0.45 \pm 0.17	0.09 \pm 0.01	3.57 \pm 0.30
10G-24	2.38 \pm 0.07	0.72 \pm 0.18	0.28 \pm 0.09	0.24 \pm 0.04	0.13 \pm 0.01	3.77 \pm 0.22
10G-25	2.51 \pm 0.12	0.99 \pm 0.07	0.47 \pm 0.30	0.34 \pm 0.08	0.31 \pm 0.11	4.58 \pm 0.27
10G-26	1.45 \pm 0.78	0.45 \pm 0.03	0.34 \pm 0.06	0.46 \pm 0.04	0.21 \pm 0.01	2.95 \pm 0.21
10G-30	2.45 \pm 0.09	0.61 \pm 0.003	0.24 \pm 0.02	0.62 \pm 0.06	0.19 \pm 0.08	4.10 \pm 0.04
10G-34	2.16 \pm 0.31	0.91 \pm 0.03	0.32 \pm 0.04	0.54 \pm 0.13	0.14 \pm 0.02	3.96 \pm 0.17
10G-36	7.41 \pm 0.1	0.74 \pm 0.13	0.42 \pm 0.13	0.92 \pm 0.07	0.19 \pm 0.12	9.66 \pm 0.04
10G-37	1.94 \pm 0.03	0.69 \pm 0.05	0.38 \pm 0.001	0.34 \pm 0.01	0.29 \pm 0.11	3.65 \pm 0.05
10G-42	1.23 \pm 0.1	0.27 \pm 0.07	0.09 \pm 0.03	0.14 \pm 0.02	0.07 \pm 0.06	1.78 \pm 0.20
10G-48	1.45 \pm 0.32	0.34 \pm 0.11	0.17 \pm 0.03	0.28 \pm 0.07	0.13 \pm 0.02	2.43 \pm 0.50
10G-58	1.46 \pm 0.04	0.55 \pm 0.06	0.13 \pm 0.04	0.13 \pm 0.02	0.18 \pm 0.08	2.45 \pm 0.20
10G-61	3.45 \pm 0.15	1.08 \pm 0.08	0.45 \pm 0.09	0.76 \pm 0.02	0.43 \pm 0.01	6.14 \pm 0.18
10G-64	4.29 \pm 0.13	0.49 \pm 0.11	0.45 \pm 0.05	0.81 \pm 0.07	0.24 \pm 0.10	6.24 \pm 0.20
10G-65	3.49 \pm 0.13	0.85 \pm 0.22	0.46 \pm 0.22	0.80 \pm 0.21	0.24 \pm 0.10	5.83 \pm 0.28
10G-68	1.72 \pm 0.01	0.61 \pm 0.08	0.21 \pm 0.04	0.17 \pm 0.01	0.18 \pm 0.06	2.89 \pm 0.05
10G-71	2.31 \pm 0.14	0.85 \pm 0.13	0.37 \pm 0.01	0.42 \pm 0.09	0.30 \pm 0.02	4.25 \pm 0.20
10G-75	2.83 \pm 0.06	0.78 \pm 0.02	0.42 \pm 0.04	0.54 \pm 0.05	0.24 \pm 0.04	4.82 \pm 0.07
10G-78	0.93 \pm 0.02	0.13 \pm 0.02	0.05 \pm 0.02	0.09 \pm 0.06	0.06 \pm 0.04	1.27 \pm 0.09
10G-80	0.93 \pm 0.03	0.27 \pm 0.01	0.05 \pm 0.005	0.05 \pm 0.01	0.07 \pm 0.02	1.37 \pm 0.06

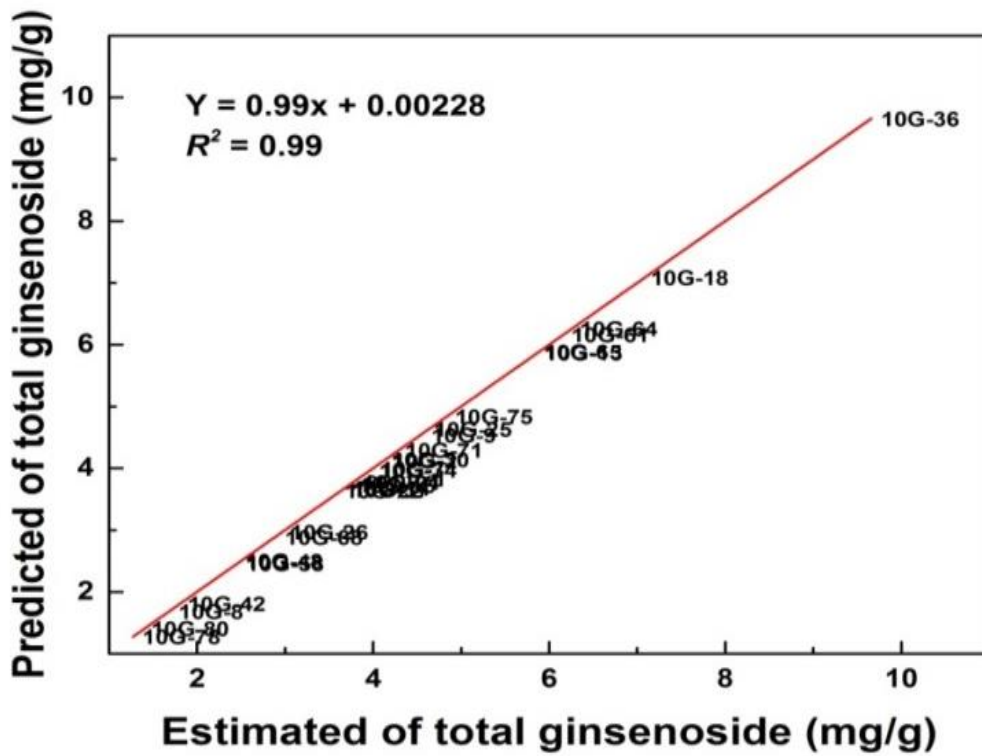


Figure 9. Linear regression plot between predicted and estimated values of total ginsenoside content of 10Gy mutant ginseng. The PLS regression model from FT-IR spectral data and estimated total ginsenoside content by HPLC analysis. Regression formula and coefficient ($R^2=0.99$) are displayed.

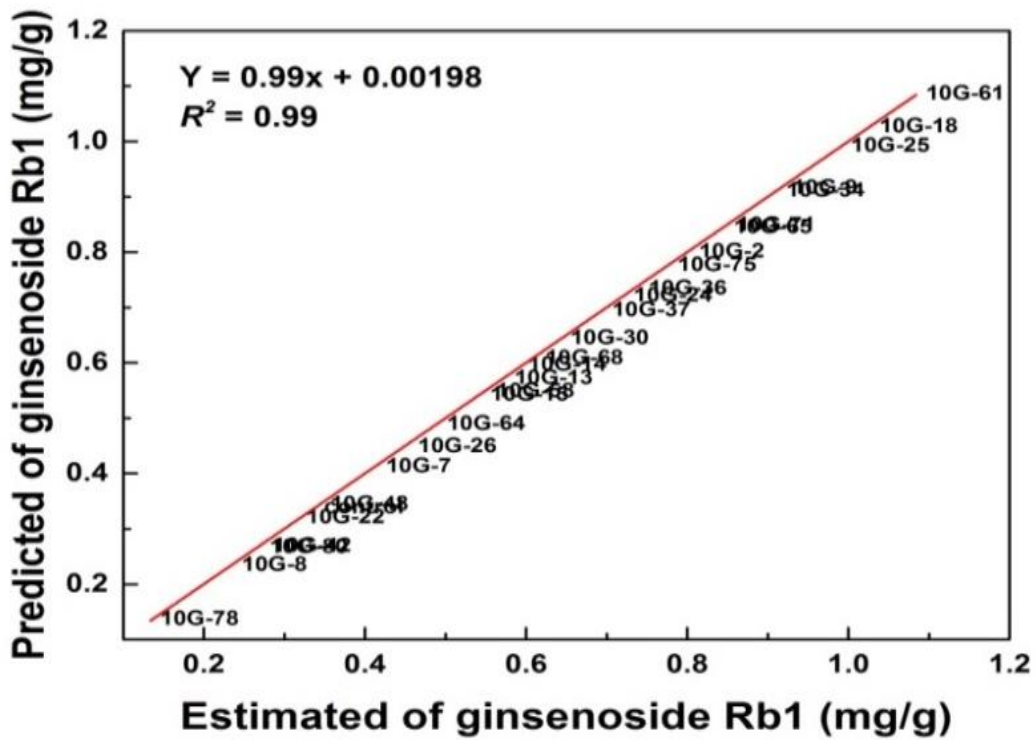


Figure 10. Linear regression plot between predicted and estimated values of ginsenoside Rb1 content of 10Gy mutant ginseng. The PLS regression model from FT-IR spectral data and estimated total ginsenoside content by HPLC analysis. Regression formula and coefficient ($R^2=0.99$) are displayed.

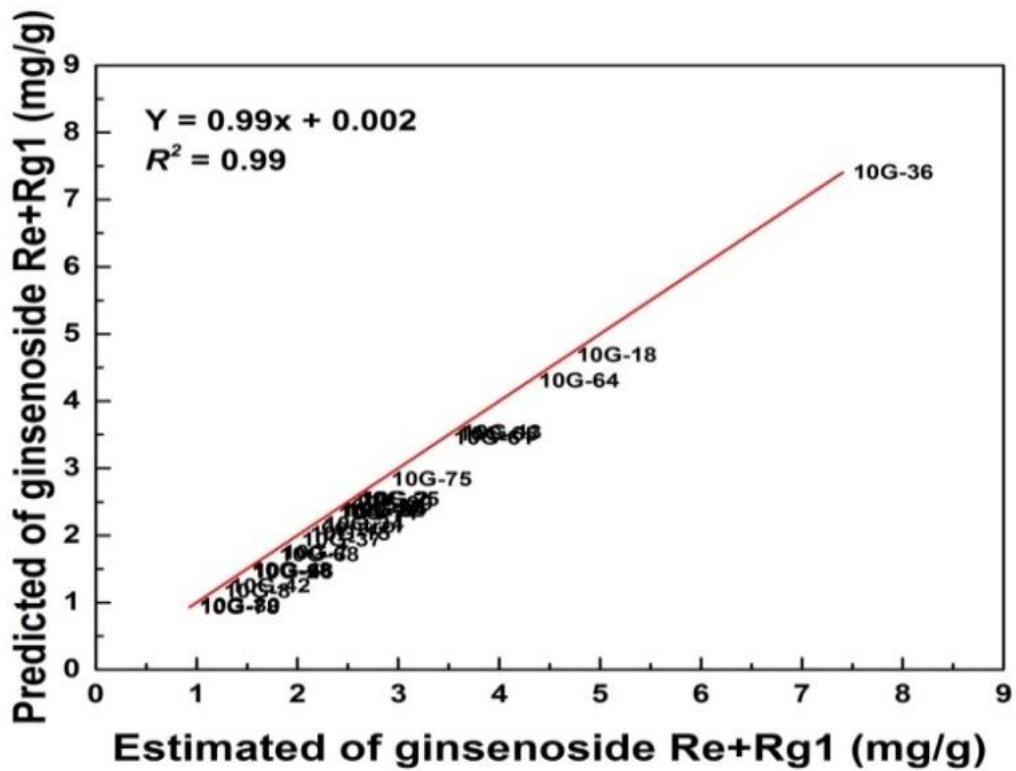


Figure 11. Linear regression plot between predicted and estimated values of ginsenoside Re+Rg1 content of 10Gy mutant ginseng. The PLS regression model from FT-IR spectral data and estimated total ginsenoside content by HPLC analysis. Regression formula and coefficient ($R^2=0.99$) are displayed.

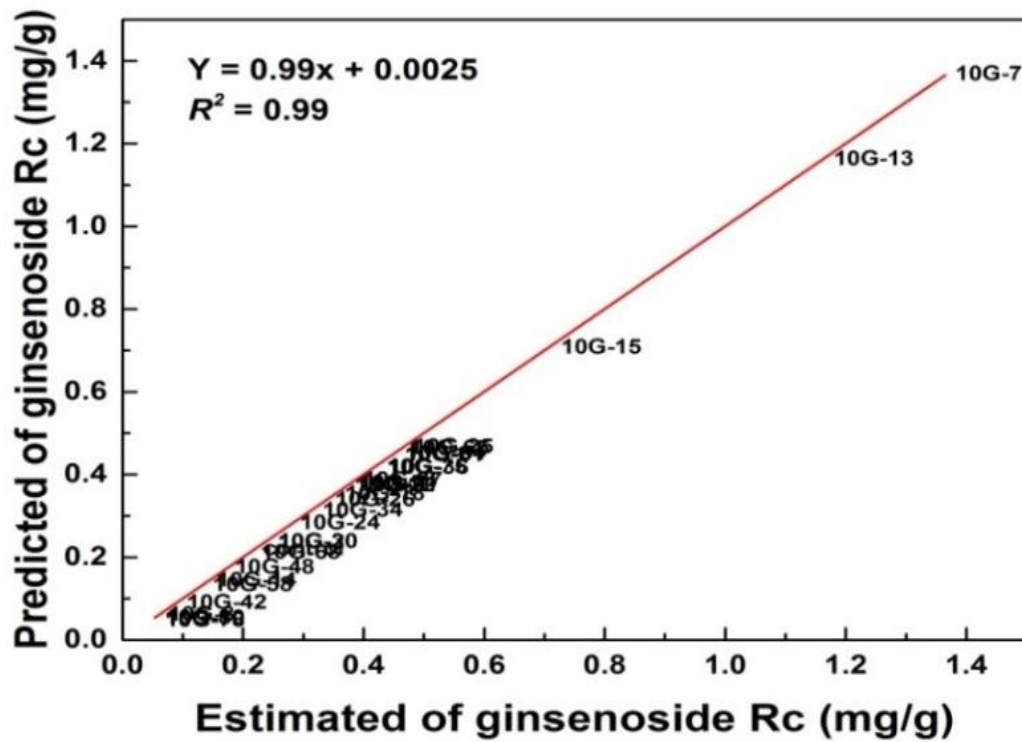


Figure 12. Linear regression plot between predicted and estimated values of ginsenoside Rc content of 10Gy mutant ginseng. The PLS regression model from FT-IR spectral data and estimated total ginsenoside content by HPLC analysis. Regression formula and coefficient ($R^2=0.99$) are displayed.

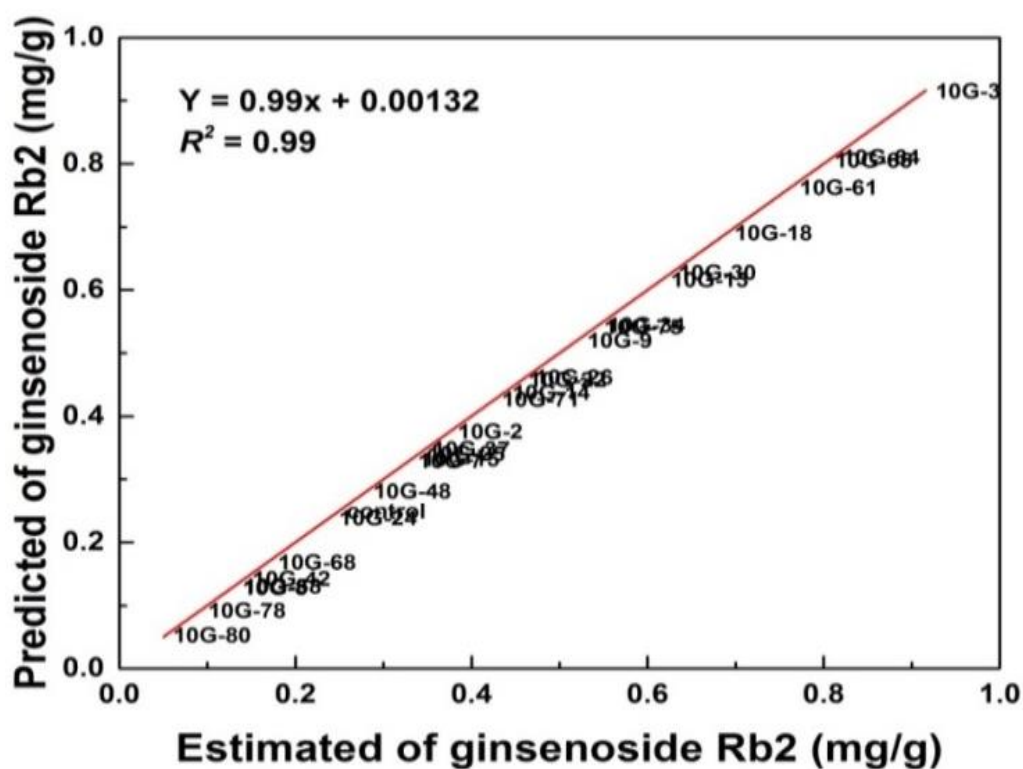


Figure 13. Linear regression plot between predicted and estimated values of ginsenoside Rb2 content of 10Gy mutant ginseng. The PLS regression model from FT-IR spectral data and estimated total ginsenoside content by HPLC analysis. Regression formula and coefficient ($R^2=0.99$) are displayed.

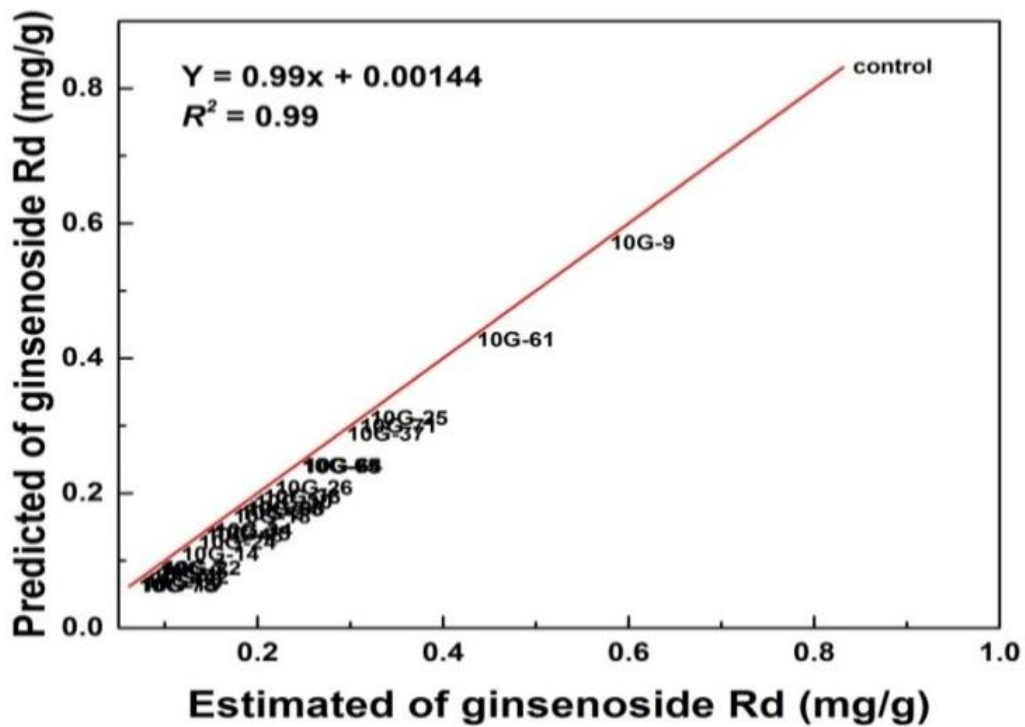


Figure 14. Linear regression plot between predicted and estimated values of ginsenoside Rd content of 10Gy mutant ginseng. The PLS regression model from FT-IR spectral data and estimated total ginsenoside content by HPLC analysis. Regression formula and coefficient ($R^2=0.99$) are displayed.

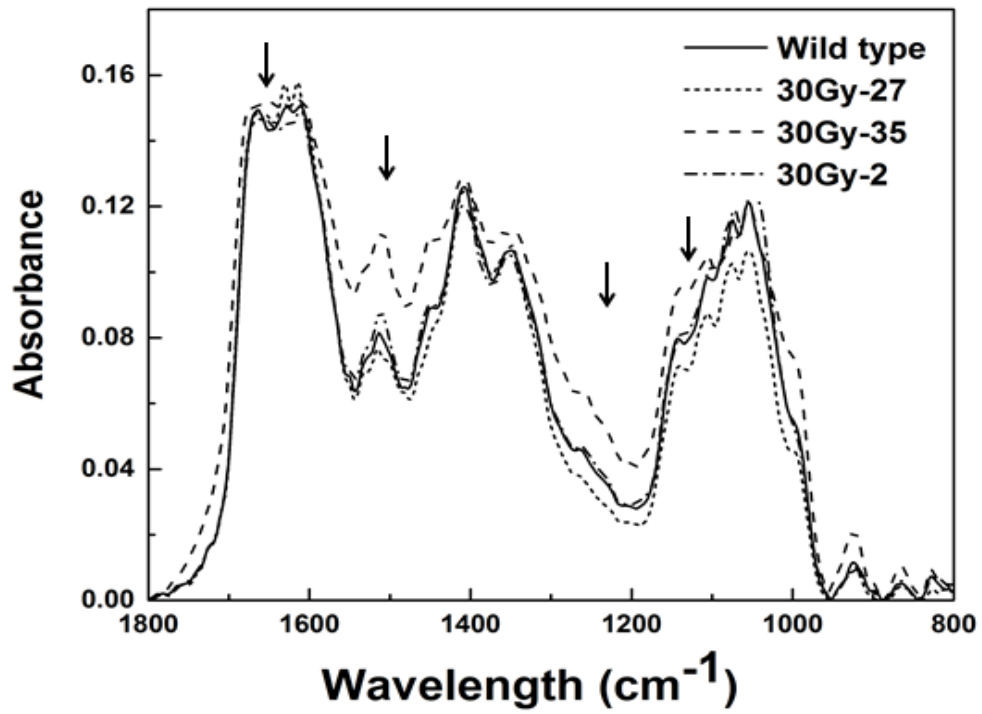


Figure 15. Representative FT-IR spectrum from 30Gy radiation mutant lines and wild type. Dotted and dashed lines represent 30Gy mutant lines and arrows display the FT-IR regions showing significant spectral variations.

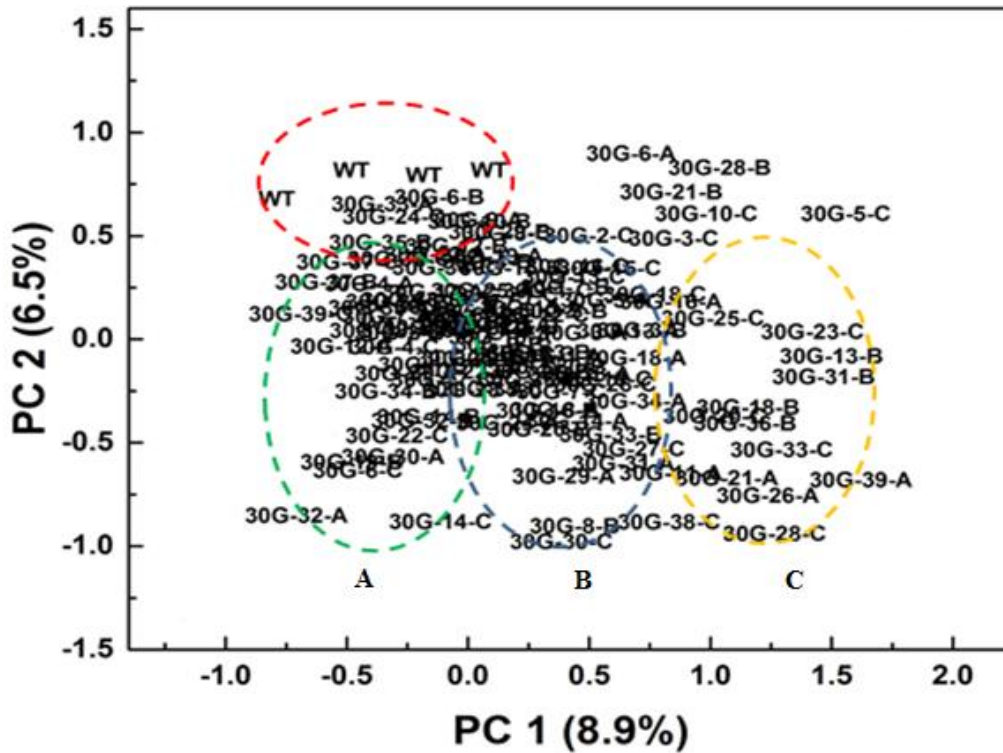


Figure 16. Two-dimensional PCA score plot of FT-IR spectral data from 30Gy radiation mutant lines and wild type. Dotted eclipses represent the clustering boundary of ginseng samples with high (30Gy-A part), medium (30Gy-B part) and low (30Gy C-part) contents of total ginsenoside. Abbreviations in the PCA score plots represent each ginseng samples.

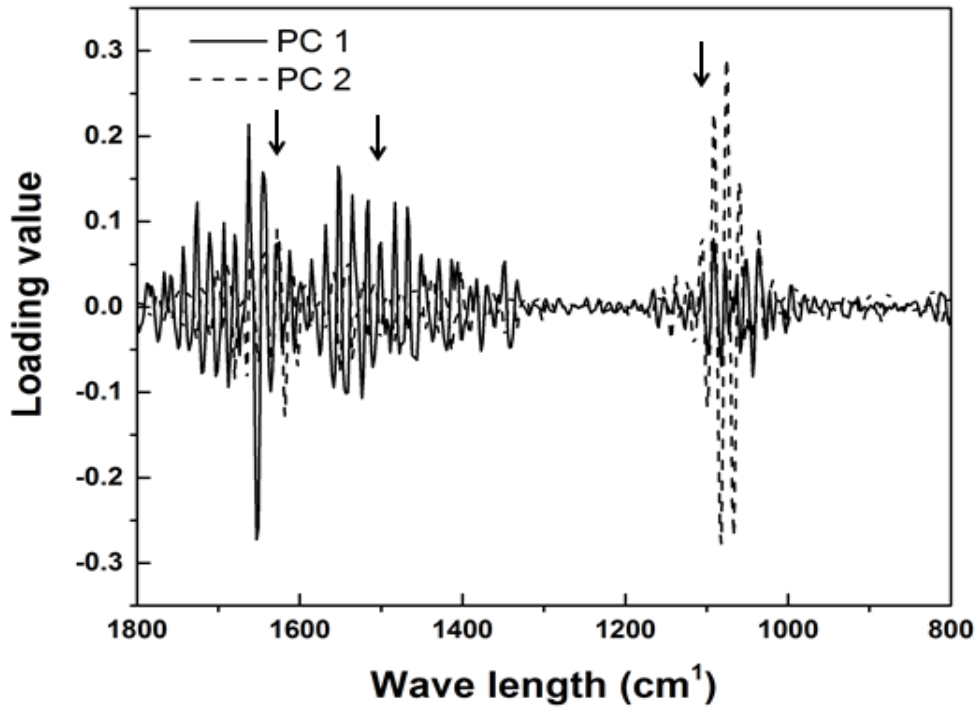


Figure 17. PC loading values plot based on PCA score plot data of 30Gy radiation mutant lines and wild type. The solid line represents the PC1 score and dotted line represents the PC 2 score. Arrows indicate the FT-IR regions which play important roles in ginseng mutant lines.

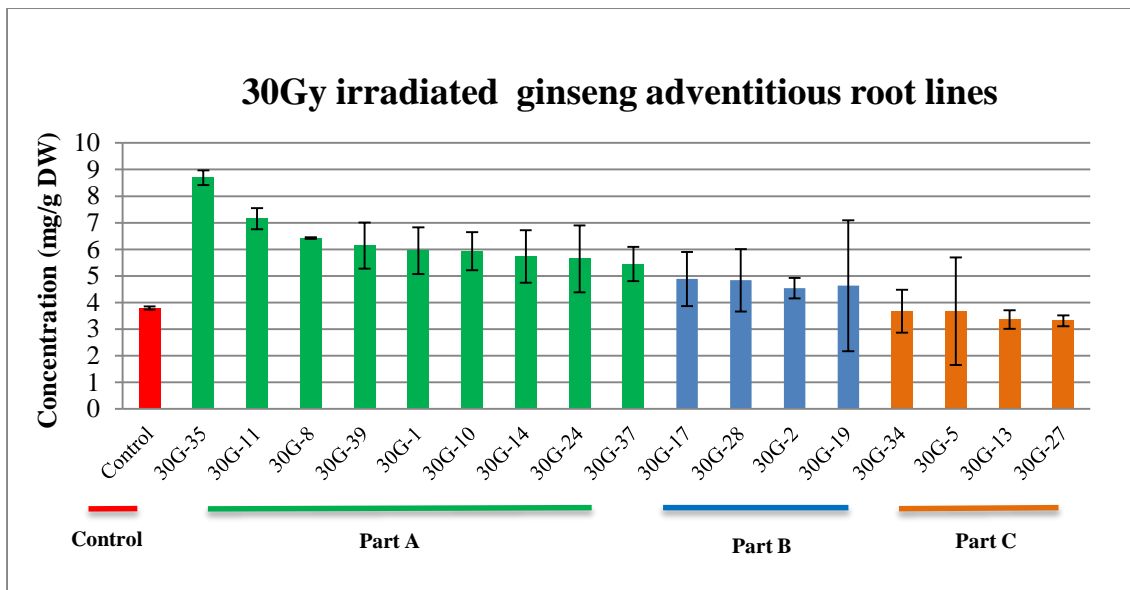


Figure 18. Determination of ginsenoside contents from 30Gy mutant lines and wild type control by HPLC analysis. Bars refer to \pm SD mean.

Table 4. Ginsenoside contents of 30Gy mutagenized ginseng cell lines as determined by HPLC. Data represent the mean±SD from three independent experiments.

Ginsenoside (mg g ⁻¹ DW)						
Mutant line	Re+Rg1	Rb1	Rc	Rb2	Rd	Total ginsenoside
30G-10	3.62±0.47	0.61±0.16	0.27±0.1	1.05±0.06	0.38±0.03	5.93±0.71
30G-1	3.83±0.46	0.74±0.16	0.25±0.07	0.98±0.25	0.15±0.03	5.95±0.88
30G-11	4.45±0.11	0.99±0.18	0.35±0.07	1.17±0.07	0.2±0.05	7.15±0.4
30G-13	2.41±0.25	0.40±0.11	0.12±0.05	0.30±0.07	0.13±0.02	3.36±0.35
30G-14	3.44±1.14	0.68±0.44	0.25±0.13	1.08±0.76	0.29±0.04	5.74±0.99
30G-17	3.24±0.68	0.58±0.02	0.19±0.04	0.58±0.05	0.29±0.3	4.89±1.02
30G-2	2.86±0.11	0.69±0.1	0.24±0.06	0.63±0.1	0.12±0.06	4.54±0.39
30G-24	3.91±1.28	0.72±0.08	0.22±0.05	0.64±0.1	0.15±0.07	5.65±1.26
30G-19	3.31±1.99	0.57±0.34	0.19±0.14	0.42±0.02	0.14±0.03	4.63±2.46
30G-37	3.39±0.1	0.81±0.28	0.28±0.11	0.77±0.25	0.19±0.1	5.44±0.64
30G-5	2.50±1.25	0.23±0.08	0.14±0.03	0.75±0.87	0.05±0.02	3.67±2.02
30G-27	2.12±0.05	0.54±0.09	0.13±0.03	0.41±0.13	0.11±0.03	3.31±0.21
30G-28	2.64±0.04	1.35±1.14	0.15±0.04	0.62±0.13	0.08±0.07	4.84±1.17
30G-34	2.36±0.35	0.46±0.17	0.14±0.07	0.58±0.25	0.12±0.03	3.67±0.81
30G-35	5.18±0.10	1.67±0.1	0.42±0.09	1.09±0.17	0.34±0.01	8.69±0.27
30G-39	3.43±1.09	0.97±0.08	0.46±0.04	1.06±0.29	0.23±0.05	6.14±0.86
30G-8	3.75±0.1	0.93±0.03	0.41±0.05	0.97±0.12	0.36±0.16	6.43±0.03

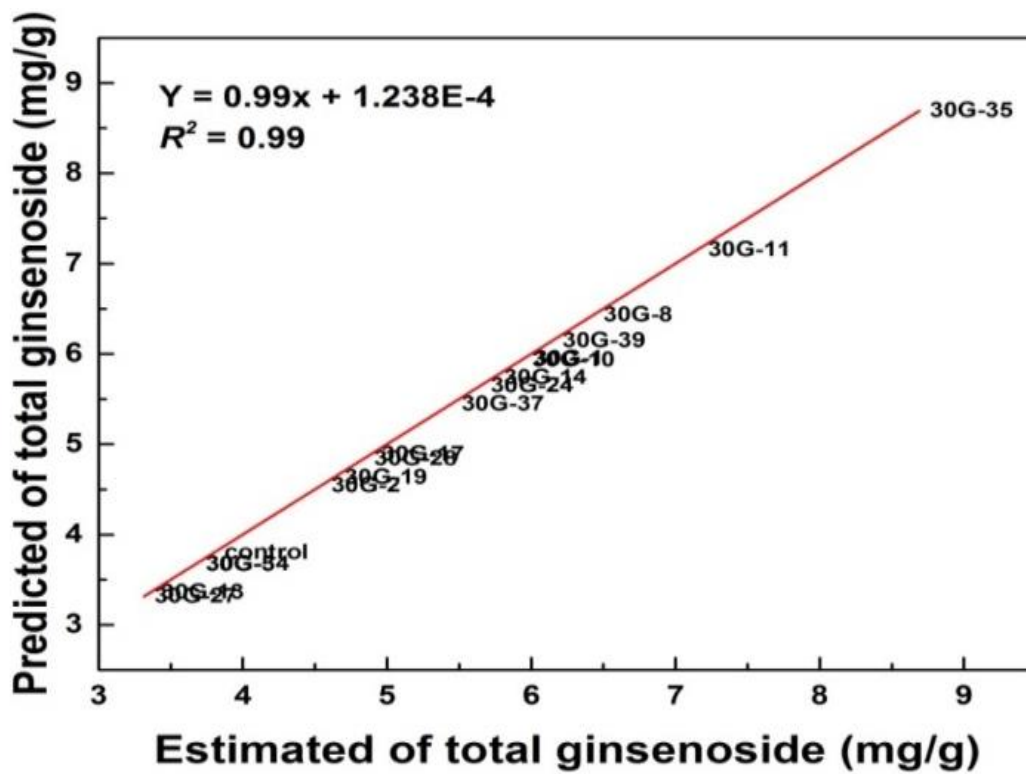


Figure 19. Linear regression plot between predicted and estimated values of total ginsenoside content of 30Gy mutant ginseng. The PLS regression model from FT-IR spectral data and estimated total ginsenoside content by HPLC analysis. Regression formula and coefficient ($R^2=0.99$) are displayed.

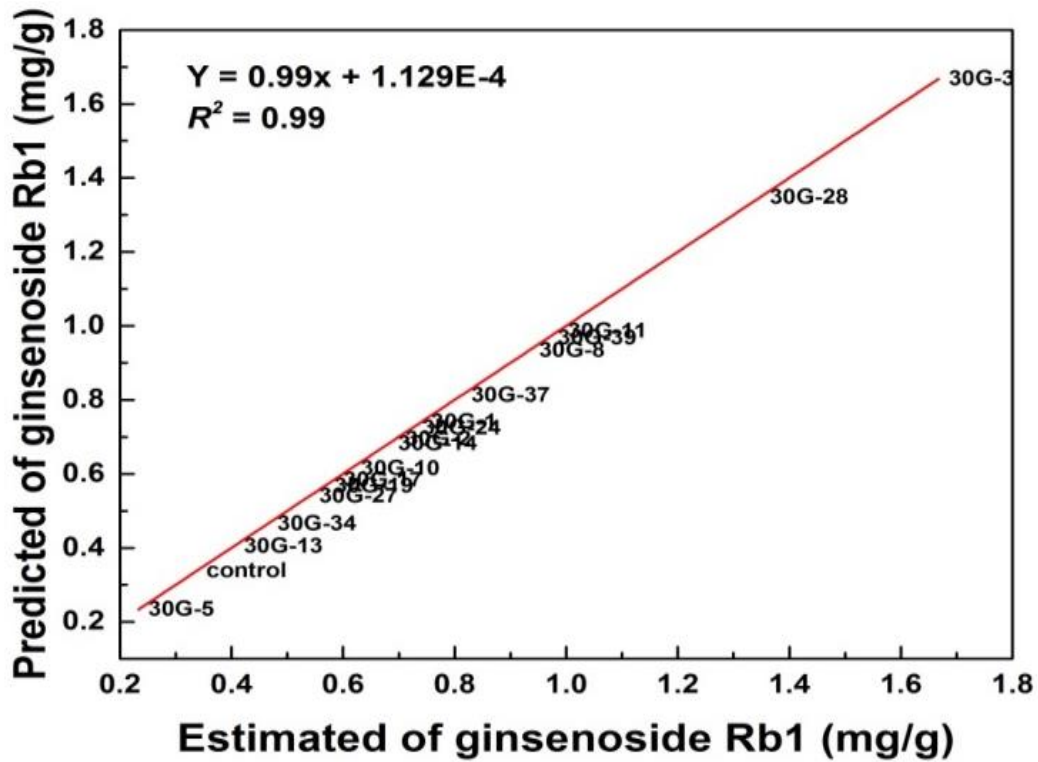


Figure 20. Linear regression plot between predicted and estimated values of ginsenoside Rb1 content of 30Gy mutant ginseng. The PLS regression model from FT-IR spectral data and estimated total ginsenoside content by HPLC analysis. Regression formula and coefficient ($R^2=0.99$) are displayed.

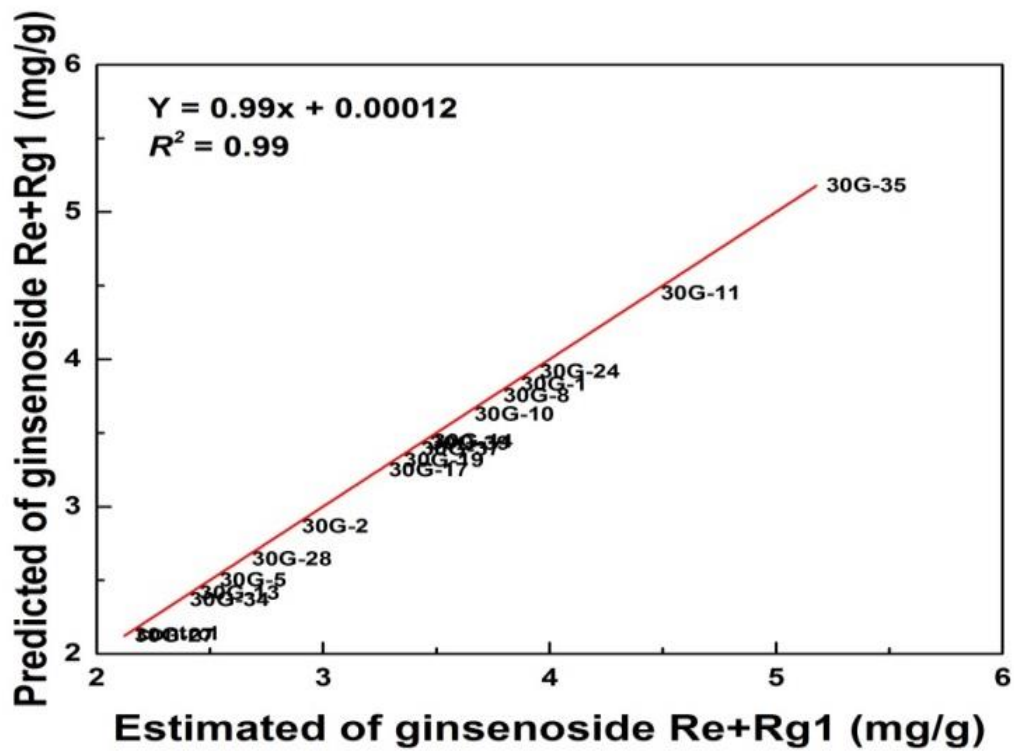


Figure 21. Linear regression plot between predicted and estimated values of ginsenoside Re+Rg1 content of 30Gy mutant ginseng. The PLS regression model from FT-IR spectral data and estimated total ginsenoside content by HPLC analysis. Regression formula and coefficient ($R^2=0.99$) are displayed.

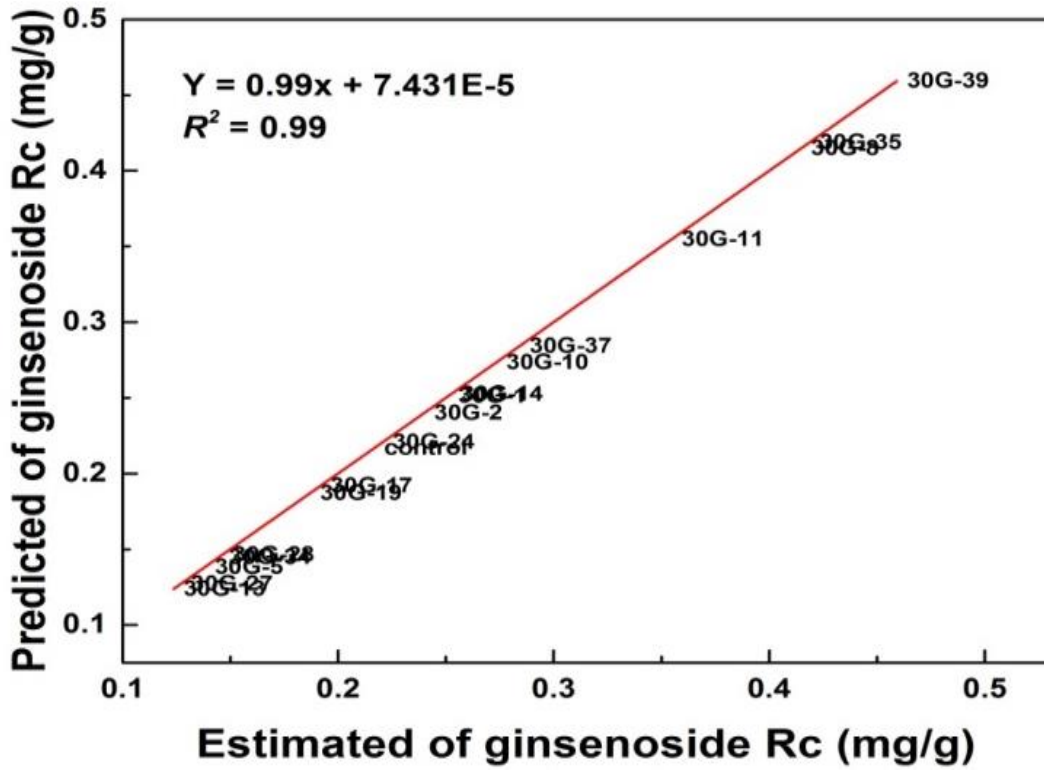


Figure 22. Linear regression plot between predicted and estimated values of ginsenoside Rc content of 30Gy mutant ginseng. The PLS regression model from FT-IR spectral data and estimated total ginsenoside content by HPLC analysis. Regression formula and coefficient ($R^2=0.99$) are displayed.

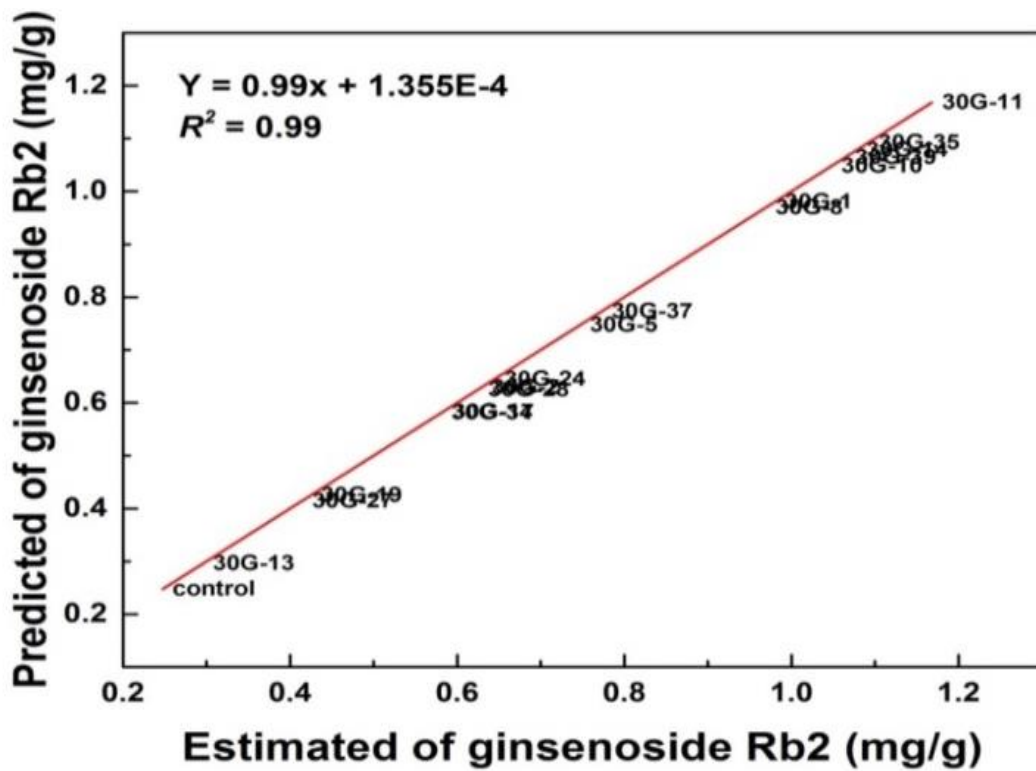


Figure 23. Linear regression plot between predicted and estimated values of ginsenoside Rb2 content of 30Gy mutant ginseng. The PLS regression model from FT-IR spectral data and estimated total ginsenoside content by HPLC analysis. Regression formula and coefficient ($R^2=0.99$) are displayed.

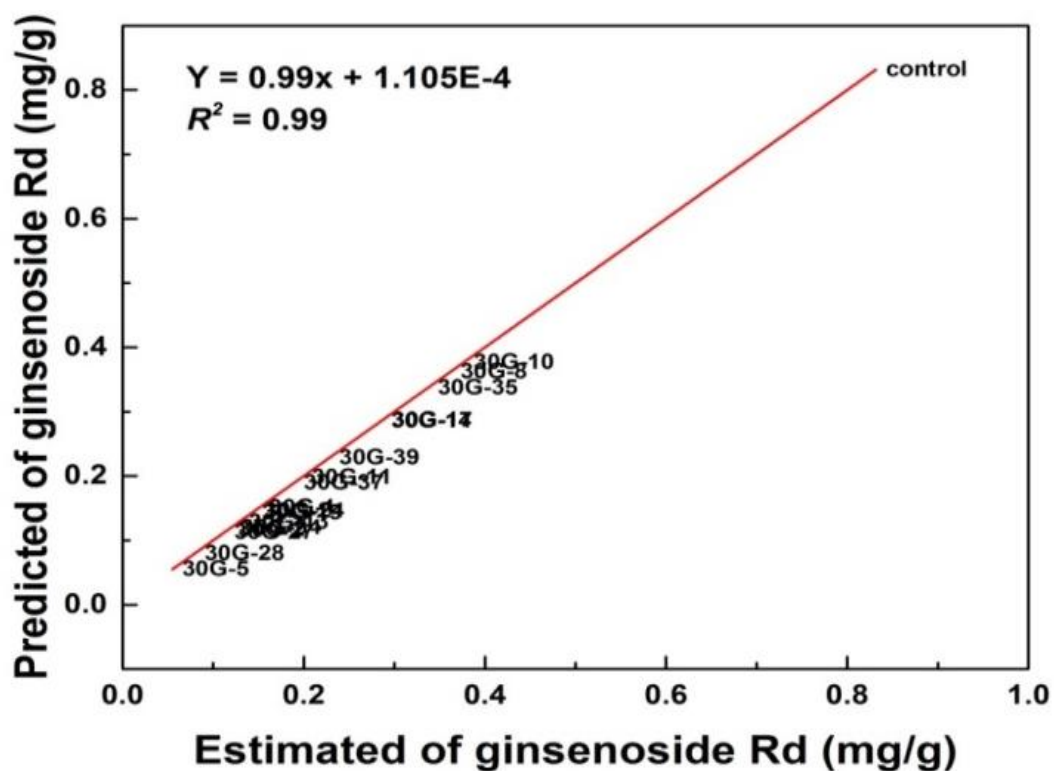


Figure 24. Linear regression plot between predicted and estimated values of ginsenoside Rd content of 30Gy mutant ginseng. The PLS regression model from FT-IR spectral data and estimated total ginsenoside content by HPLC analysis. Regression formula and coefficient ($R^2=0.99$) are displayed.

CONCLUSION

Ginseng is a perennial herb and belongs to the Araliaceae family. Seven major species of ginseng are spread throughout East Asia, Central Asia, and North America.

The wide chemical assortment of both triterpenoid and steroidal saponins has become renewed interest and examinations of these compounds in recent years as potential chemotherapeutic agents.

The quantitative prediction modeling of ginsenoside content from ginseng cell lines were developed using PLS regression algorithm from FT-IR spectra. The regression coefficients between predicted and estimated values of 10Gy and 30Gy mutagenized ginsenoside Re+Rg1, Rb1, Rc, Rb2, Rd and total ginsenoside content were 0.99, respectively. These results indicate that FT-IR spectroscopy, in combination with multivariate analysis, can be used to predict the ginsenoside content in ginseng cell lines with high precision. The proposed method can be used for mutation breeding of *Panax ginseng* as a rapid selection tool.

REFERENCE

- Ananthaswamy HN, Vakil UK, Screenvasan A (1970) Effect of gamma radiation on wheat starch and its components. *Journal of Food Science* 35: 795-798.
- Ayed N, Yu HL, Lacroix M (1999) Improvement of anthocyanin yield and shelf-life extension of grape pomace by gamma irradiation. *Food Research International* 32: 539-543.
- Briskin DP (2000) Medicinal plants and phytomedicines. Linking plants biochemistry and physiology to human health. *Plant physiology* 124: 507-514.
- Charlesby A (1981) Crosslinking and degradation of polymers. *Radiation Physiology Chemistry* 18: 59-66.
- Chen L, Carpita NC, Reiter W-D, Wilson RH, Jeffries C, McCann MC (1998) A rapid method to screen for cell-wall mutants using discriminant analysis of Fourier transform infrared spectra. *Plant J* 16: 385-392.
- Chen Y, Xie MY, Yan Y, Zhu SB, Nie SP, Li C, Wang YX, Gong XF (2008) Discrimination of *Ganoderma lucidum* According to Geographical Origin with Near Infrared Diffuse Reflectance Spectroscopy and Pattern Recognition Techniques. *Analytica Chimica Acta* 618: 121-130.
- Chew OS, Hamdan MR, Ismail Z, Ahmad MN (2004) Assessment of Herbal Medicines by Chemometrics-Assisted Interpretation of FTIR Spectra. *Analytica Chimica Acta* 570: 116-123.
- Choi KM, Kwon JH, Sung H, Ban SH, Yang DC (2002) Production of Ginsenoside in hairy roots irradiated by ^{60}Co γ -ray on *Panax ginseng* C.A.Meyer. *Journal of Ginseng research* 26(4): 219-255.

Deschreider AP (1960) Changes in starch and its degradation products on irradiating wheat flour with gamma rays. *Starch-Starke* 12: 197-200.

Fuzzati N, Gabetta B, Jayakar K, Pace R, Peterlongo F (1999) Liquid chromatography electrospray mass spectrometric identification of ginsenoside in *Panax ginseng* roots. *Journal of Chromatography A* 854(1-2): 69-79.

Fuzzati N (2004) Analysis method of ginsenoside. *Journal of Chromatography* 812: 119-133.

Han J, Choi Y (2009) Rapid induction of *Agrobacterium tumefaciens*-mediated transgenic roots directly from adventitious roots in *Panax ginseng*. *Plant Cell, Tissue and Organ Culture* 96: 143-9.

Joseph R, Yeoh HH, Loh CS (2004) Induced mutations in cassava using somatic embryos and the identification of mutant plants with altered starch yield and composition. *Plant Cell Reports* 23: 91-98.

Ketchum REB, Gibson DM, Croteau RB, Shuler ML (1999) The kinetics of taxoid accumulation in cell suspension cultures of *Taxus* following elicitation with methyl jasmonate. *Biotechnology & Bioengineering* 62: 97-105.

Kim YS, Hahn EJ, Yeung EC, Paek KY (2003) Lateral root development and saponin accumulation as affected by IBA or NAA in adventitious root cultures of *Panax ginseng* C.A. Meyer. *In Vitro Cell Dev Biol Plant* 39: 245-249.

Kim SW, Ban SH, Chung H, Cho SH, Chung HJ, Choi PS, Yoo OJ, Liu JR (2004) Taxonomic discrimination of higher plants by multivariate analysis of Fourier transform infrared spectroscopy data. *Plant Cell Rep* 23: 246-250.

Kim DS, Lee IS, Jang CS, Kang SY, Seo YW (2005) Characterization of the altered anthranilate synthase in 5-methyltryptophan-resistant rice mutants. *Plant Cell Rep* 24: 357–365.

Kim O, Bang K, Kim Y, Hyun D, Kim M, Cha S (2009) Upregulation of ginsenoside and gene expression related to triterpene biosynthesis in ginseng hairy root cultures elicited by methyl jasmonate. *Plant Cell, Tissue and Organ Culture* 98: 25-33.

Kim DS, Kim SY, Jeong IY, Kim JB, Lee GJ, Kang SY, Kim W (2009) Improvement of ginsenoside production by *Panax ginseng* adventitious roots induced by γ -irradiation. *Biol Plant* 53: 408-414.

Kim DS, Song M, Kim SH, Jang DS, Kim JB, Ha BK, Kim SH, Lee KJ, Kang SY, Jeong IY (2013) The improvement of ginsenoside accumulation on *Panax ginseng* as a result of γ -irradiation. *J Ginseng Res* 37: 332-340.

Kovalchuk I, Molinier J, Yao Y, Arkhipov A, Kovalchuk O (2007) Transcriptome analysis reveals fundamental differences in plant response to acute and chronic exposure to ionizing radiation. *Mutat Res* 624: 101–113.

Kwon JH, Bélanger JMR, Paré JRJ, Yaylayan VA (2003) Application of the microwave-assisted process (MAPTM) to the fast extraction of ginseng saponins. *Food Research International* 36: 491-8.

Kwon YK, Jie EY, Sartie A, Kim DJ, Liu JR, Min BW, Kim SW (2015) Rapid metabolic discrimination and prediction of dioscin content from African yam tubers using Fourier transform-infrared spectroscopy combined with multivariate analysis. *Food Chemistry* 166: 389-396.

- Lai YH, Ni YN, Kokot S (2010) Classification of Raw and Roasted Semen Cassiae Samples with the Use of Fourier Transform Infrared Fingerprints and Least Squares Support Vector Machines. *Applied Spectroscopy* 64: 649-656.
- Lui D, Li YG, Xu H, Sun SQ, Wang ZT (2008) Differentiation of the root of Cultivated Ginseng, Mountain Cultivated Ginseng and Mountain Wild Ginseng using FT-IR and two-dimensional correlation IR spectroscopy. *Journal of Molecular Structure* 883-884: 228-235.
- Mallol A, Cusido RM, Palazon J, Bonfill M, Morales C, Pinol MT (2001) Ginsenoside production in different phenotypes of *Panax ginseng* transformed roots. *Phytochemistry* 57: 365-371.
- Mokobia CE, Okpakorese EM, Analogbei C, Agbonwanegbe J (2006) Effect of gamma irradiation on the grain yield of Nigerian *Zea mays* and *Arachis hypogaea*. *Journal of Radiological Protection* 26: 423-427.
- Park JY, C. Y. Lee CY, Won JY (2007) Analytical optimum of ginsenoside according to the gradient elution of mobile phase in high performance liquid chromatography. *Korean Journal of Medicinal Crop Science* 15(3): 215-219.
- Peigen, X. (1989) General status on ginseng research in China. *Herbal Pol* 35: 69-72.
- Rakwal R, Agrawal GK, Shibato J, Imanaka T, Fukutani S, Tamogami S, Endo S, Sahoo SK, Masuo Y, Kimura S (2009) Ultra low-dose radiation: stress responses and impacts using rice as a grass model. *Int J Molecular Science* 10: 1215-1225.
- Shibata S (2001) Chemistry and cancer preventing activities of ginseng saponins and some related triterpenoid compounds. *Journal of Korean Medical Science* 16.
- Shim M, Lee YJ (2009) Ginseng as a complementary and alternative medicine for postmenopausal symptoms. *Journal of Ginseng Research* 33: 89-92.

Sivakumar G, Yu KW, Paek KY (2005) Production of biomass and ginsenoside from adventitious roots of *Panax ginseng* in bioreactor cultures. *Eng Life Sci* 5: 333-342.

Song SY, Jie YJ, Ahn MS, Kim DJ, Kim IJ, Kim SW (2014) Discrimination of African yams containing high functional compounds using FT-IR fingerprinting combined by multivariate analysis and quantitative prediction of functional compounds by PLS regression modeling. *Kor J Hort Sci Technol* 32: 105-114.

Song SY, Lee YK, Kim IJ (2016) Sugar and acid content of *Citrus* prediction modeling using FT-IR fingerprinting in combination with multivariate statistical analysis. *Food Chemistry* 190: 1027-1032.

Sokhey AS, Chinnaswamy R (1993) Chemical and molecular properties of irradiated starches extrudates. *Cereal Chemistry* 70: 260-270.

Subhan F, Anwar N, Ahmad N, Gulzar A, Siddiq A (2004) Effect of gamma radiation on growth and yield of barley under different nitrogen levels *Pakistan Journal of Biological Science* 7: 981-3.

Vogler BK, Pittler MH, Ernst E (1999) The efficacy of ginseng: a systematic review of randomised clinical trials *Eur J Clin Pharmacol*. 55: 567–575.

Wold H (1966) Estimation of principal components and related models by iterative least squares. In: K. R. Krishnaiah (ed.). *Multivariate analysis Academic Press, New York* p. 391-420.

Wu J, Zhong JJ (1999) Production of ginseng and its bioactive components in plant cell culture: current technological and applied aspects. *J Biotechnol* 68: 89-99.

Xie JT, Attele AS, Yuan CS (2011) Ginseng beneficial potential adverse effects. *Traditional Chinese medicine* p. 57-76.

Yap KYL, Chan SY, Lim CS (2007) Authentication of Traditional Chinese Medicine Using Infrared Spectroscopy: Distinguishing between Ginseng and Its Morphological Fakes. *Journal of Biomedical Science* 14: 265-273.

Ying Z, Augustine TLT (2015) Discrimination of Wild- Grown and Cultivated *Ganoderma Lucidium* by Fourier Transform Infrared Spectroscopy and Chemometric Methods *American Journal of Analytical* 6: 480-491.

Yoshikawa T, Furuya T (1987) Saponin production by cultures of *Panax ginseng* transformed with *Agrobacterium rhizogenes*. *Plant Cell Rep* 6: 449-453.

Zhang JY, Bae TW, Boo KH, Sun HJ, Song IJ, Pham CH, Ganesan M, Yang DH, Kang HK, Ko SM et al (2011) Ginsenoside production and morphological characterization of wild ginseng (*Panax ginseng* Meyer) mutant lines induced by γ -irradiation (^{60}Co) of adventitious roots. *J Ginseng Res* 35: 283-293.

Zhang JY, Sun HJ, Song IJ, Bae TW, Kang HG, Ko SM, Kwon YI, Kim IW, Lee J, Park SY, Lim PO, Kim YH, Lee HY (2014) Plant regeneration of Korean wild ginseng (*Panax ginseng* Meyer) mutant lines induced by γ -irradiation (^{60}Co) of adventitious roots. *J Ginseng Res* 38: 220-225.

ACKNOWLEDGEMENT

This thesis of a master degree has been achieved at the Department of Biotechnology, Jeju National University, since autumn 2013. There is a handful of people who I am deeply indebted for their help and support. Therefore I would like to honor each one of them and express my sincerest gratitude in this acknowledgement.

First of all, I would like to convey my warmest gratitude to my supervisor Professor Hyo Yeon Lee, who gave me the opportunity to conduct my study in his research group, and for his guidance, generous contribution of knowledge and experience, valuable comments and encouragement from the start until the end of my study.

My deepest gratitude also goes to Professor Hyeon-Jin Sun who was very generous with his time, giving priceless knowledge and assisting me through every step of this thesis.

I thank to Dr. Seung Yeop Song and Dr. Jun Ying Zhang for guiding me through some parts of my experiment and helpful discussions on my study.

I would like to thank to Dr. Enkhchimeg Vanjildorj for guiding me to study in South Korea.

I am especially indebted to all the members in my laboratory both past and present for their good will, cooperation and assistance during my study.

I wish to offer my humble gratitude to my colleagues and friends at the Jeju National University International Students Organization for sharing me numerous coffees, lunches, and laugh at all times.

I would also like to acknowledge my family all around the world for their invaluable support and love in completing this research. I deeply cherish you all.